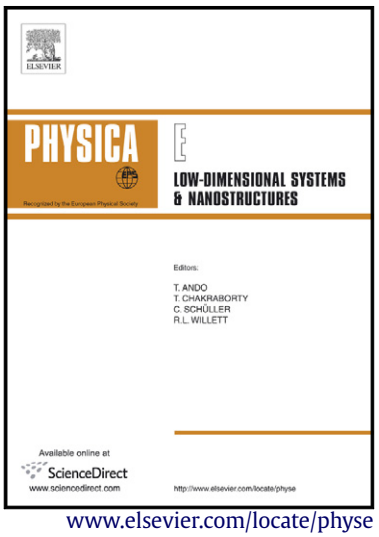

Dielectric response of II–VI semiconductor core-shell ensembles: Study of the lossless optical condition

R.M. de la Cruz, C. Kanyinda-Malu

www.elsevier.com/locate/physe

PII: S1386-9477(14)00215-X
DOI: http://dx.doi.org/10.1016/j.physe.2014.05.029
Reference: PHYSE11625

To appear in: *Physica E*

Received date: 13 May 2014
Accepted date: 29 May 2014

Cite this article as: R.M. de la Cruz, C. Kanyinda-Malu, Dielectric response of II–VI semiconductor core-shell ensembles: Study of the lossless optical condition, *Physica E,* http://dx.doi.org/10.1016/j.physe.2014.05.029

Dielectric response of II-VI semiconductor core-shell ensembles: study of the lossless optical condition

R M de la Cruz[a,1,*], C Kanyinda-Malu[b]

[a] *Departamento de Física, Universidad Carlos III de Madrid, EPS. Avda. de la Universidad 30, 28911 Leganés (Madrid), Spain*
[b] *Departamento de Economía Financiera y Contabilidad, Area de Matemáticas y Estadística, Universidad Rey Juan Carlos, FCJS, Paseo de los Artilleros s/n, 28032 Madrid, Spain*

Abstract

We theoretically investigate optical properties of II-VI core-shells distributions mixtures made of two type-I sized-nanoshells as a plausible negative dielectric function material. The nonlocal optical response of the semicondutor QD is described by using a resonant excitonic dielectric function, while the shell response is modeled with Demangeot formula. Achieving the zero-loss at an optical frequency ω; i.e., $\epsilon_{eff} = \epsilon'_{eff} + i\epsilon''_{eff}$ with $\epsilon'_{eff} < 0$ and $\epsilon''_{eff} = 0$, is of fundamental importance in nanophotonics. Resonant states in semiconductors provide a source for negative dielectric function provided that the dipole strength and oscillator density are adequeate to offset the background. Furthermore, the semiconductor offer the prospect of pumping, either optically or electrically, to achieve a gain mechanism that can offset the loss. We analyze optimal conditions that must be satisfied to achieve semiconductor-based negative index materials. By comparing with II-VI semiconductor quantum dots (QDs) previously reported in the literature, the inclusion of phonon and shell contributions in the ϵ_{eff} along with the finite barrier Effective Mass Approximation (EMA) approach, we found similar qualitative behaviours for the ϵ_{eff}. The lossless optical condition along with $\epsilon'_{eff} < 0$ are discussed in terms of sizes, volume fractions and embedding medium of the mixtures distributions. Furthermore, we estimated

*Corresponding author
Email addresses: rmc@uc3m.es (R M de la Cruz), clement.kanyindamalu@urjc.es (C Kanyinda-Malu)
[1]Phone: +34 91 624 8733,Fax: +34 91 624 8749

optical power to maintain nanocrystals density in excited states and this value is less to that previously obtained in II-VI semiconductor QDs.

Keywords: Optical properties, II-VI core-shells distributions, Maxwell-Garnett theory, lossless optical materials.
PACS: 78.67.Bf, 78.30.Fs, 78.40.Fy

1. Introduction

Semicondutor quantum dots (QDs) nanocrystals, have attracted considerable interest owing to their unique optical and electrical properties, which are governed by the composition, dimensions and shape of each of their components. Through the choice of specific materials, one can tailor the confinement potential profile, giving rise to the popularly known as "'wave function engineering"'. This wave function engineering has opened route to colloidal core-shell nanocrystals (NCs) in which the alignment of energy states at the interface between two semicondutors promotes spatial localization of electrons and holes in core and/or shell regions. Each localization regime gives rise to different optical behaviours. For example, in type-I regime where electrons and holes are localized in the core region, NCs exibit bright and stable fluorescence that is used for biological tagging and as emitters in light-emitting diodes. Meanwhile, the type-II regime NCs, where electrons are confined in the core region while holes are localized in the shell regions, exbit intrinsic charge separation which is beneficial for photovoltaic applications [1, 2, 3].

In addition, overcoated II-VI NCs have been observed to improve the PL quantum yields trough the passivation of the surface nonabsorbing recombination sites. However, despite their high emission efficiencies, there are significant challenges to practical applications of NCs in lasing technologies. Because of the degeneracy of the lowest-energy emitting levels, population inversion in NCs can only be achieved if the average number of excitons per nanocrystal is greater than 1. That implies that at least some of the NCs must contain multiexcitons. It is known that a significant complication arising from the multiexctonic nature of the optical amplification in NCs is the efficient non-radiative Auger recombination induced by confinement of exciton-exciton interactions. One of the strategies for solving the problem of Auger decay consists in developping structures that allow realization of optical gain, where generation of photons by stimulated emission dominates

over photon absorption [4, 5]. Optical gain requires population inversion, that is, the situation in which the number of electrons in the excited state is greater than that in the ground state. The attempt to develop QDs NCs with suppressed non- radiative Auger recombination gave rise to the development of giant QDs NCs where small CdSe core were surrounded by thick CdS shell [6, 7].

On the other hand, the possibility of creating optical negative index metamaterials (NIM) and espilon-near-zero (ENZ) materials using nanostructured metal-dielectric composites has triggered intense basic and applied researches over the past several years [8, 9]. Much efforts are dedicated to the engineering and extension of the functionalities of metarials at optical frequencies, specically to design NIM or ENZ in the visible range of electromagnetic spectrum (see for example refs. [8, 10, 11]). Most of these attempts take advantage of plasmonic behaviour of noble metals such silver and gold in addition to dielectric bulk materials to design arrays of NIM thin films composite materials. In this context, a suitable design of metal-based composite requires both positive and negative permitivities to compensate the lossy behaviours of many systems [12, 13]. With the emergence of qunatum dots, silver coated core-shell NCs have been also employed to compensate the gain emission of QDs [14] and to obtain a negative-refractive index material.

Previously, Webb et al. [15] and Fu et al. [16] later on, have proposed semiconductor QDs mixture as a lossless negative dielectric constant optical material. To do, Webb et al. [15] first deduced a mascroscopic dielectric function for a single QD within a density-matrix approach, where the excitonic susceptibility is averaged over the confined volume of QDs. In that treatment, the QD exciton energy was derived from the Effective Mass Approximation (EMA) with an infinite potential barrier and without taking into account the phonons contribution, nor the shell effect in the homogenized II-VI semiconductor QD dielectric function. In the cited work, following their previous theoretical studies [17], they suggested that, to achieve negative ϵ'_{eff}, the gain must occur at higher energy. However, later on, Fu et al. [16] demostrated that negative ϵ'_{eff} may be achieved, unlike the gain is associated to lower or higher energy using a set of two types of QDs.

To characterize most of these nanocomposites, researchers have used a variety of optical measurements as well as some structural techniques. The challenge of tailoring the QDs distribution size, the shell thickness and surface electronic properties through physical or chemical methods has deserved a great attention in the field of nanotechnology [18, 19, 20, 21, 22, 23, 24, 25].

Available theoretical models for QDs optical properties range from the formalism of light scattering of small particles based on polarizability of dielectric spheres to more sophisticated calculations [26, 27, 28]. The effects of charge carriers confinement on the self-polarization of the electron-hole pairs (excitons) in QDs, were reported in spherical and non-spherical QDs. In many of these studies, the incorporation of the size-dependent functions is made following generalized Penn's model [29], or by including spatially smooth dielectric functions at the QD-surrounding material's interface [27]. In metallic nanoparticles for example, the effect of size on the dielectric function is often introduced through the size-dependent damping coefficient that accounts on different scattering mechanisms such as electron-electron, electron-phonon, surface and defect interactions [30].

On the other hand, the Maxwell-Garnett (MG) effective medium theory has proved to be a good model for the optics of semiconductor inclusions in glasses [31] and many other homegeneous media. Also, when a good description of dielectric functions of small sized particles is known, the generalization of MG with the mixing rules, can be applied to investigate the optical properties of mixing distributions of nanoshells.

This theory is also appropriate when the inclusions are made of two-component spheres such as core-shell NCs [32]. A natural extension of this generalization can be made to investigate the optical properties of a medium consisting in a mixing distributions of nanoshells. These mixing distributions will take into account the size inhomogeneity, through inequal sized-cores QD dimensions to reach typical features in the growth of real dispersive nanostructures.

In our previous work, the visible (VIS) and infrared (IR) spectra of isolated II-VI semiconductor nanoshells revealed a size-dependent behaviour as a consequence of the size-quantum confinement effect [33]. At this end, we used the effective dielectric function of QD that acounts on size-quantization of the QD-polarization produced by the ground-state exciton excited by an electromagnetic field [15, 16].

Then, the aim of the present work is to investigate the dielectric function of exciton polariton in a mixture of spherical II-VI semiconductor core-shell NCs of type I (excitons confined in the core), where we assume the EMA approach with finite potential barrier and considering the phonons contribution along with the shell effect in the effective dielectric function. Besides, we present the influence of gain on the homogenized dielectric constant in order to describe the required core-shell density and pumping to achieve the

lossless condition. We analyze optimal conditions that must be satisfied, to achieve semiconductor-based negative index materials. For the investigated systems, specific volume fractions and core-shells sizes along with the embedding media effects have been found to determine the lossless condition.

The paper is organized as follows. In section 2, an outline of extended MG theory applied in mixing distributions of core-shell NCs is given. The implementation of the model in typical II-VI semiconductor nanoshells distributions along with a discussion of the results are given in section 3. The main remarks and conclusion of this work will be given in section 4.

2. Maxwell-Garnett effective medium approach and core-shell NCs

Let us model a II-VI semiconductor core-shell NC as a coated sphere with inner radius R_c and outer radius R_s ($R_s > R_c$) embedded in a homogeneous medium with a positive real dielectric constant ϵ_e. Core and shell materials are characterized by frequency-dependent dielectric functions ϵ_c and ϵ_s, respectively.

Within the context of effective medium approach, if the radiation wavelength is much greater than the nanoparticle radius, we can consider the coated spherical QD as an effective homogeneous sphere whose equivalent dielectric function depends on the core (ϵ_c) and shell (ϵ_s).

In type I core-shell NCs, the bandgap of the shell material is larger than that of the core. Therefore, both electrons and holes are confined in the core, giving rise to the exciton localization in the core region.

To determine ϵ_c we adopt the electric-dipole approximation as described by Webb el al. [15] to account on quantum confinement effect on the total QD dielectric function. In addition, we include a bulk-like phonon contribution where the size-dependent damping terms are neglected. With these assumptions, the total dielectric function in the core region can be described by

$$\epsilon_c(\omega) = \epsilon_{\infty,c} + \frac{8e^2}{V_c\epsilon_0 m_{ex,c}}\left[\frac{2\rho - 1}{{\omega_{ex,c}}^2 - \omega^2 - i2\omega\gamma}\right] + \epsilon_{\infty,c}\left[\frac{\omega_{LO,c}^2 - \omega^2}{\omega_{TO,c}^2 - \omega^2 - i\gamma_{ph}\omega}\right]. \quad (1)$$

Here, $\omega_{TO,\,c}$ and $\omega_{LO,\,c}$ are the core transverse and longitudinal optical phonons frequencies, with γ_{ph} its damping constant. $m_{ex,c}$, $\omega_{ex,c}$ and ρ represent respectively, exciton reduced mass, exciton energy ($E_c = \hbar\omega_{ex,c}$), and the av-

eraged probability of the single exciton being in ground state. In section 3, we summarize further materials parameters that are used to describe the dilectric response of the ensemble of QDs NCs.

Since ϵ_c depends on the exciton energy, we calculated the electron and hole energies using EMA in a finite barrier potential, while the Coulomb interaction is treated as a perturbative correction to the confinement energies, so that the exciton energies take into account the finite boundary conditions at the interface. For more details, see ref. [34].

Writing the complex dielectric function of the shells as a bulk-like semiconductor dielectric function with plasmons and phonons contributions [35]; i.e.,

$$\epsilon_s(\omega) = \epsilon_{\infty,s}\left[1 + \frac{\omega_{LO,s}^2 - \omega^2}{\omega_{TO,s}^2 - \omega^2 - i\gamma_{ph}\omega} - \frac{{\omega_p}^2}{\omega^2 + i\gamma\omega}\right] \tag{2}$$

the effective core-shell dielectric function ϵ_{ns} can be expressed within the framework of the electrostatic dipole approximation, in a similar way as described in ref. [32]; that is

$$\frac{\epsilon_{ns} - \epsilon_e}{\epsilon_{ns} + 2\epsilon_e} = \frac{(\epsilon_s - \epsilon_e)(\epsilon_c + 2\epsilon_s) + (R_c/R_s)^3(\epsilon_c - \epsilon_s)(\epsilon_e + 2\epsilon_s)}{(\epsilon_s + 2\epsilon_e)(\epsilon_c + 2\epsilon_s) + 2(R_c/R_s)^3(\epsilon_c - \epsilon_s)(\epsilon_s - \epsilon_e)}. \tag{3}$$

Looking at the core-shell NCs as polarizable point dipoles, the effective dielectric function of the composite medium is described for an ensemble of two distributions of NCs using an extended Maxwell-Garnett effective approach; i.e.,

$$\frac{\epsilon_{eff} - \epsilon_e}{\epsilon_{eff} + 2\epsilon_e} = f_1\frac{\epsilon_{ns,1} - \epsilon_e}{\epsilon_{ns,1} + 2\epsilon_e} + f_2\frac{\epsilon_{ns,2} - \epsilon_e}{\epsilon_{ns,2} + 2\epsilon_e} = Q. \tag{4}$$

By solving the multiphase nanoshell distributions in eq. 4 for ϵ_{eff} and introducting two-type distributions effective dielectic funtions, being f_1 and f_2 the volume fractions of the two distributions, respectively, we find that

$$\epsilon_{eff} = \frac{\epsilon_e(1 + 2Q)}{1 - Q}. \tag{5}$$

The right-side term in eq. 5, includes both nanoshell model parameters, together with boundary-conditions applied to a binary mixture of two kinds of nanoshells as solution of Laplace equation. The latter expression follows

the formalism discussed by Fu et al. [16], in which we replaced two single QDs by two core-shell species. We analyze the dielectric response of these binary mixed NCs through the frequency-dependent real and imaginary parts of the effective dielectric function in order to derive the lossless conditions as a function of strcutural parameters. Lossless conditions require $\epsilon''_{eff} = 0$ and negative index condition is related to $\epsilon'_{eff} < 0$. From the eq. 5, we find that the lossless condition is achieved when $Q'' = 0$.

On the other hand, by combining simultaneously the lossless condition and the $\epsilon'_{eff} < 0$, we find that negative index condition can be reached if $Q' > 1$ or $Q' < -1/2$ at the same lossless resonant frequency, that is, the frequency at which ϵ''_{eff} vanishes.

As the right-side mixed term Q in eq. 4 is a complex-valued expression that depends on different model parameters, such as, the fraction volume, core and shell radii, embedding medium dielectric constants, confinement-like regimes, one can easily tailor a negative index metamaterial by accomodating each of these parameters to the best conditions of device-design engineering. In our case, we will focus our attention on structural and compositional parameters such as volume fractions and shell-sized materials. However, the key requirement to reach lossless materials or negative-index metamaterials lay on the coexistence of lossy and gain constituents in layered-like structures of NCs devices.

3. Results and discussion

To illustrate our results, we numerically analyze a binary mixture of CdSe/ZnS spherical nanoshells, half of which providing gain and half having loss absorptions, using an extended MG formalism. The gain and loss features are introduced through the probability transition parameter ρ in ϵ_c (see eq. 1), taking values < 0.5 for gain and > 0.5 for lossy constituents in the mixture [15].

In contrast to many researchers (see for example ref. [36]), we do not include a metallic shell to compensate gain emission of QDs NCs. Instead, the shell dielectric function is introduced with its phonons and plasmonic damping terms (see eq.2). For sake of comparison, we considered polymer and semiconductor as host material to analyze the effect of emdedding medium, with respectively $\epsilon_\infty = 2.3$ (polyethylene (PE)) and 10.0 (semiconductor).

The choice of CdSe/ZnS mixture core-shells QDs in the simulation is dictated by the fact that CdSe/ZnS colloidal core-shell microcavities present

a fast experimental development of its optical gain, as reported elsewhere [16, 37]. Indeed, the polymer-coated QDs are widely used for its stability in comparison with QDs coated with small organic ligands. In addition, it was shown that with the use of polymers, multiple and diverse chemical functionalities can be introduced at the surface of QDs.

The effects of core sizes and volume fractions are analyzed in order to determine the numerical lossless optical conditions. In addition, we estimate the minimum optical energy pumping required to maintain NCs in excited states in analogy with the work of Fu et al. [16]. Shell thicknesses of 3 $ML = 0.93\ nm$ and 2 nm are considered in good agreement with experimental and theroretical works reported elsewhere. In table 1, we summarize values of structural constants used in the numerical simulations. Most of these values are taken from refs.[38, 39, 40, 41].

Table 1: II-VI semiconductors structural parameters used in the calculations, where ω_p and γ_{ph} are fixed to 69.7 cm^{-1} and 8.5 cm^{-1}, respectively.

Parameters	E_g eV	ϵ_∞	ω_{LO} (cm^{-1})	ω_{TO} (cm^{-1})	m_e^* (m_0)	m_h^* (m_0)	γ (cm^{-1})
CdSe	1.769	6.2	213.1	165.2	0.19	0.8	56.4
ZnS	3.54	5.2	349	269	0.4	0.525	56.4

Throughout all the work, the gain resonance is assumed to be at $\hbar\omega_{ex,c} - \hbar\delta$, where $\hbar\omega_{ex,c}$ is the loss resonance and $\hbar\delta$ is the energy difference achieved through a small reduction in core-shell size, which should satisfy $\hbar\delta > \hbar\gamma$. That is, adjustable values of ρ satisfying gain-resonances are assigned to smaller core-sizes NCs constituents, while absorption-like values of that parameter are assigned to bigger NCs. Equal loss and gain volume fractions are assumed for both kinds of NCs to obtain the same weight in the MG expression.

Figure 1 shows ϵ_{eff} for gain and absorptive distributions with different sizes. For the three investigated cases, the core radius of the gain distribution is maintained constant with a fixed value of 3 nm, while the core radius of the absorptive distribution is considered to be 4 nm, 5 nm and 6 nm, respectively. We find that the gain resonance is localized approximately at 1.4 eV, while the loss resonances are localized at 1.49 eV, 1.43 eV and 1.415 eV for the distributions of 4 nm, 5 nm and 6 nm, respectively. As we mentioned above, the loss and gain resonances do not correspond exactely with the single excitons energies of the two distributions because of the complex weighting

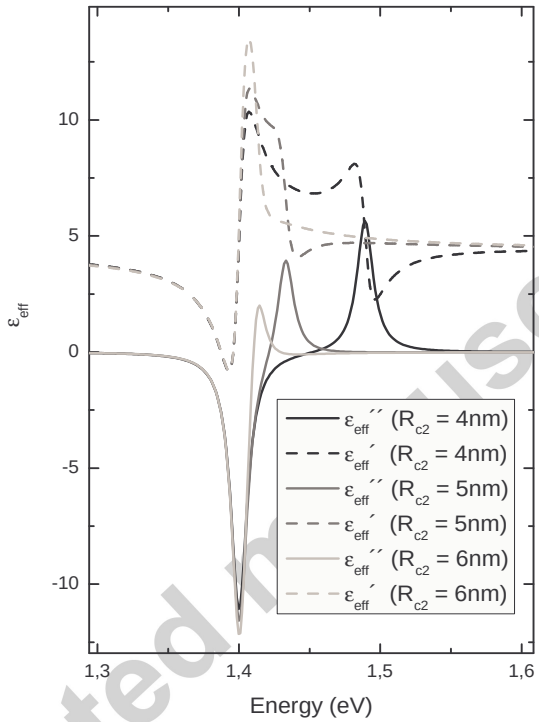

Figure 1: *Effective dielectric function of CdSe/ZnS/PE characterized by gain distributions with R_{c1} = 3 nm and varying loss distributions sizes: R_{c2} = 4, 5 and 6 nm respectively. The shell thickness is fixed to 3 ML and volume fractions $f_1 = f_2 = 0.2$.*

in the denominator of the MG formalism. Similar behaviours of gain and loss resonances were previously reported by Fu et al. [16] in PbSe/ZnSe QDs mixtures for $\hbar\delta \leq 3\, meV$. The lossless optical condition ($\epsilon_{eff} = 0$) is achieved for the three sized distributions in a small range of energies. However, this range seems to be reduced to an unique value for the absorptive distributions with 5 nm and 6 nm sizes. Also, at the gain resonance, ϵ'_{eff} is negative in the three investigated distributions.

In order to investigate in depth possible effects of the distributions sizes on ϵ_{eff}, we turn our attention to the dependences of $\hbar\delta$ and energies separation between loss and gain resonances on the geometrical factor of R_{c1}/R_{c2} (see figure 2). While $\hbar\delta$ decreases with radii ratio, gain and loss peaks separation energies tend to increase before they fall down for higher values of radii ratio.

On the other hand, we also investigate the effects of shell thicknesses on ϵ_{eff}. Figure 3 shows the dielectric response of NCs ensemble for two shell sizes of 0.93 nm and 2 nm, with equal volume fractions of 0.2 and core radii of 3 and 5 nm, respectively. The increase in the shell thickness produces energy shifts in both resonant peaks of the investigated structure. With a greater thickness, we observe that the gain and loss resonances energy separation is reduced to $\approx$ 30 meV (gain resonance at 1.47 eV and loss resonance at 1.50 eV). Also, negative values in ϵ_{eff} are observed for smaller shell sizes, while it remains positive with higher values of the shell sizes (see dashed plots in fig. 3) over all investigated frequencies.

To complete the effects of a large number of adjustable parameters in the model, we also investigate the role of volume fractions and embedding material on the lossless optical condition. Figure 4 shows ϵ_{eff} for 3 nm and 4 nm sized gain and loss distributions, respectively with volume fractions of $f_1 = f_2 = 0.05$; $f_1 = f_2 = 0.1$ and $f_1 = f_2 = 0.2$. When the volume fraction increases, which means a greater core-shells density, the loss- and gain-resonance peaks separation becomes smaller. This reduction in peak energies separation restricts the extension of lossless optical region and gives rise to an abrupt change in the sign of ϵ''_{eff}. With respect to the volume fractions, we found that reaching $\epsilon'_{eff} < 0$ at the gain resonances requires a minimum concentration of core-shells in the distributions to be pumped. Figure 5 depicts the effects of the embedding material on ϵ_{eff} for gain and absorptive distributions. The semiconductor surrounding medium with its large dielectric constant ($\epsilon_\infty = 10$) produces a more negative ϵ'_{eff} at the gain resonance. In addition, the lossless optical condition is fullfilled at nearly an inflexion point determined by an unique frequency value. These two features

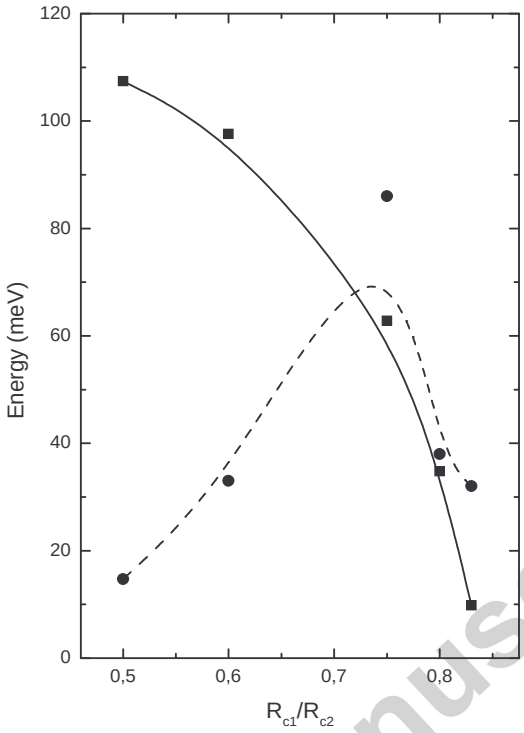

Figure 2: *Dependences of $\hbar\delta$ (square symbol) and energy difference of loss and gain resonances (circle symbol) versus the radii ratio of the two distributions. The solid and dashed lines are guide for the eyes.*

are also obtained with a higher concentration of core-shell NCs (see figure 4). Similar dependences on volume fractions and embedding media on ϵ_{eff} were previously reported in CdSe QDs [15].

As can be derived from the above simulation results, the condition $\epsilon'_{eff} < 0$ together with the lossless condition can be achieved for particular NCs adjustable parameters. For instance, for distributions with $R_{c1} = 3\,nm$, $R_{c2} = 6\,nm$, the above conditions are satisfied for $f_1 = f_2 = 0.3$, when $Q' > 1$. Figure 6 shows the behaviour of ϵ_{eff} for this particular case. Similarly, Bratkovsky et al. [42] have found that, in a metal wire/QD composite metamaterial, the way to obtain negative dielectric function consists in increasing the volume fraction of the gain material as high as 0.3. Therefore, we can infer that the core-shells sizes, volume fractions and embedding medium in mixtures of gain and loss distributions are crucial factors if one wants to control the lossless

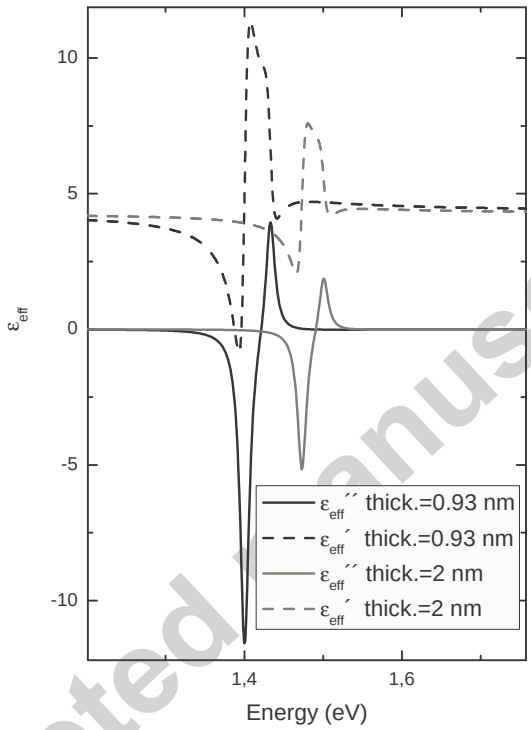

Figure 3: *Effective dielectric function for CdSe/ZnS/PE binary mixtures with R_{c1} = 3 nm (gain), R_{c2} = 5 nm (loss), shells thicknesses equal to 3 ML = 0.93 nm and 2 nm, respectively and volume fractions $f_1 = f_2 = 0.2$.*

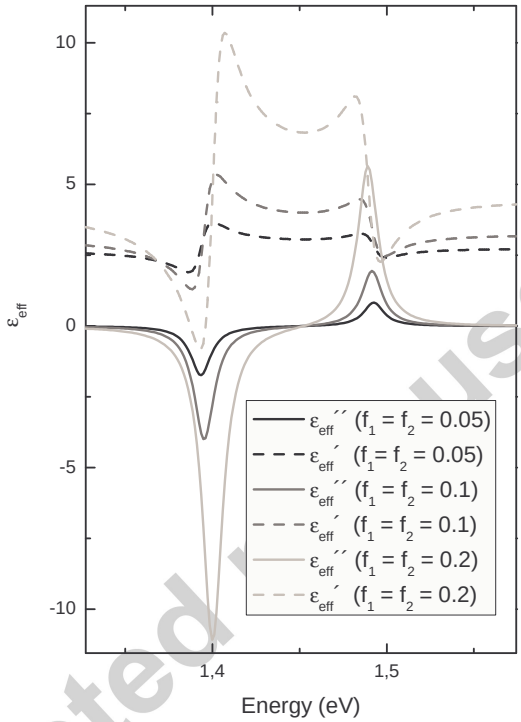

Figure 4: *Effective dielectric function for CdSe/ZnS/PE mixtures distributions characterized by $R_{c1} = 3$ nm (gain), $R_{c2} = 4$ nm (loss), shells thicknesses equal to 3 ML and volume fractions $f_1 = f_2 = 0.05$; $f_1 = f_2 = 0.1$ and $f_1 = f_2 = 0.2$, respectively.*

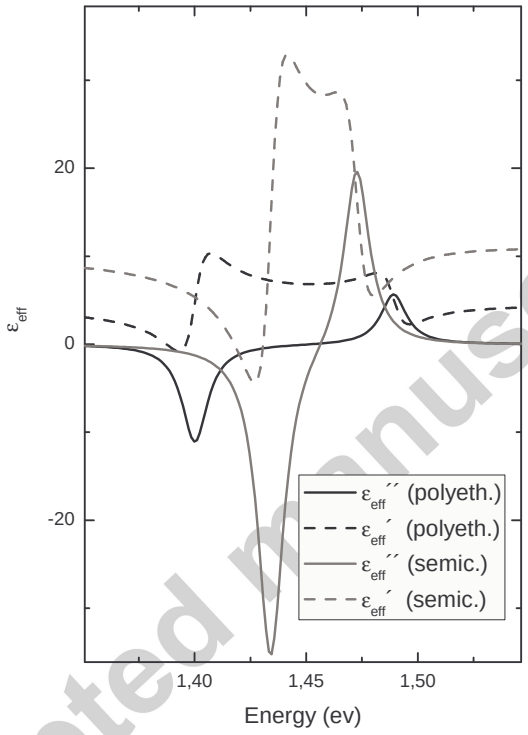

Figure 5: *Effective dielectric function for CdSe/ZnS distributions embedded in PE and semiconductor, respectively and characterized by R_{c1} = 3 nm (gain), R_{c2} = 4 nm (loss), shells thicknesses equal to 3 ML and volume fractions $f_1 = f_2 = 0.2$.*

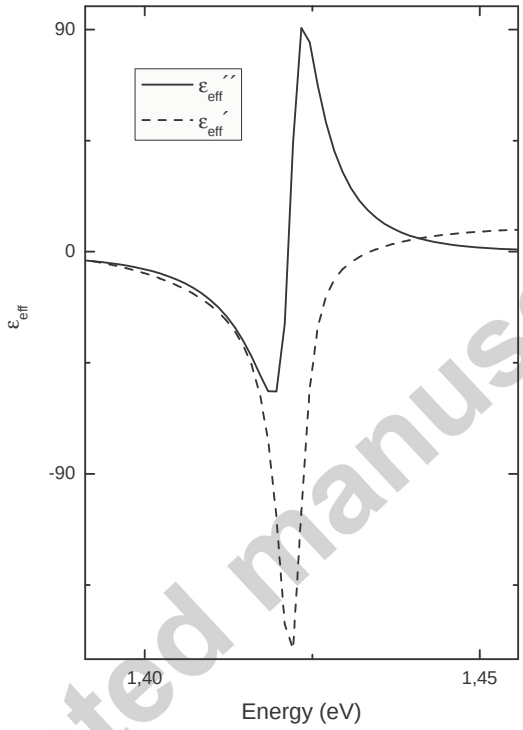

Figure 6: *Effective dielectric function for CdSe/ZnS/PE characterized by gain distributions of R_{c1} = 3 nm and loss distributions of R_{c2} = 6 nm respectively, shells thicknesses equal to 3 ML and volume fractions $f_1 = f_2 = 0.3$.*

optical conditions and the possibility to obtain negative dielectric function optical material.

Now, we will estimate the minimum optical power (P) to maintain N core-shells NCs in excited states, where $P = N\hbar\omega/2\tau$ [43], being τ the core-shells spontaneous radiative emission decay. For core-shell CdSe/ZnS NCs, the radiative recombination of singlet trion at 300 K is between 8 and 10 ns [44]. Then, the required optical power becomes $8.8{\times}10^6$ W.cm^{-3} when the core-shells density is around $7.86{\times}10^{17} cm^{-3}$; i.e., $R_s = 3.93\ nm$ and $f = 0.2$, while $\hbar\omega = 1.405\ eV$ is the energy when $\epsilon''_{eff} = 0$. For example, for a film of thickness of 10 μm and a cross section of 1 mm^2, this corresponds to an averaged optical power of 88 W. As another example, in a waveguide with a cross section of 10 μm^2 and 100 μm of length, the absorbed power needs to be only of 8.8 mW.

To compare with an equal density of QDs; i.e., $7.86{\times}10^{17} cm^{-3}$, being τ = 3.6 ns [16], we obtain an optical power of 24.5 $\times 10^6$ W.cm^{-3}, which is approximately triple of optical power in core-shell NCs. Then, the optical pumping seems to be easier for core-shell NCs.

It is reported in the literature [44] that in typical CdSe NCs, the long photoluminescence ($\approx$ 20 ns at 300 K) is connected with the lowest excited state having a forbidden optical transition dipole (in other words, it is a "'dark state"'). However, radiative recombination of singlet trions is always optically allowed, because one of the hole spins (either spin up or down) forming the singlet can always recombine with any electron spin.

On the other hand, if we consider non-radiative decay processes via LO phonon modes, τ will be of tenth order of ns [45] and the optical power will increase significantly. Non radiative relaxation processes are given when the difference of energies between levels is very small and the time scale is shorter and shorter than the radiative transitions. In semiconductors, the electrons go down from a level of high energy to a metastable level of small energy difference, via non-raditive relaxation and then, they go down to fundamental level via radiative processes. The metastable states show interesting features for the laser fabrication. In fact, if the electrons decay slowly from the metastable states, they can be promoted to higher states with scare loss and the stimulated emission can be used to yield an optical signal.

4. Conclusions

We obtained a plausible candidate of negative dielectric function optical material by mixing distributions of CdSe/ZnS core-shells NCs (type I) with different exciton energies. We evaluated its effective dielectric function by a generalized MG theory, where the core dielectric function accounts on the carriers confinement within EMA finite barrier framework through the excitonic eigenfrequencies, while the shell dielectric function includes plasmons and phonons contributions. We observed that the shell and phonon effect on ϵ_{eff} along with the finite barrier scheme yield similar qualitative behaviours than those previously reported in mixtures of PbSe/ZnSe QDs. Core-shells sizes, volume fractions and embedding medium in mixtures distributions are crucial to control the lossless optical condition and the possibility to obtain negative dielectric function optical material. On the other hand, we estimated the optical power to maintain N core-shells NCs in excited states for radiative transitions and this value is smaller than those obtained for equivalent CdSe QDs density.

[1] I.L. Medintz, H.T. Uyeda, E.R. Goldman and H. Mattoussi, Nature Material, **4** (2005) 435.

[2] A.P. Alivisatos, V.W. Gu and C. Larabell, Annual Review of Biomedical Engineering, **5** (2005) 55.

[3] L. Sun, Y. Zang, M. Sun, H. Wang, X. Zhu, S. Xu, Q. Yang, Y. Li, and Y. Shan, Coloids Interface Sci., **350** (2010) 90.

[4] V.I. Klimov, S.A. Ivanov, J. Nanda, M. Archermann, I. Bezel, J.A. McGuire and A. Piryatinski, Nature **447** (2007) 441.

[5] F. García-Santamaría, Y. Chen, J. Vela, R.D. Schaller, J. N. Hollingsworth and V.I. Klimov, Nano Lett. **9** (2009) 3482.

[6] B.N. Pal, Y Ghost, S. Brovelli, R. Laocharaensuk, V. I. Klimov, J.A. Hollingsworth and H. Htoon, Nano Lett. **12** (2012) 331.

[7] J. Kundu, Y. Ghost, A.M. Denis, H. Htoon and J. A. Hollingworth, Nano Lett. **12** (2012) 3031.

[8] C.M. Soukoulis, S. Linden and M. Wegener, Science **315** (2007) 47.

[9] V.M. Shalaev and F. Traeger, Appl. Phys. B**84** (2006) 1.

[10] M.I. Stockman, Optics Express **19** (2011) 22029.

[11] G. Dolling, M. Wegener, C.M. Soukoulis and S. Linden, Opt. Lett. **32** (2007) 53.

[12] A. Boardman, V.V. Grimalsky, Y.S. Kivshar, S.V. Koshevaya, M. lapine, N.M.Litchinitser, V.N. Malnev, M. Noginov, Y.G. Rapoport and V.M. Shalaev, Laser Photonics Rev. (2010) 1.

[13] X. Ni, S. Ishii, M.D. Thoreson, V.M. Shalaev, S. Han, S. lee and A.V. Kildishev, Optics Express **19** (2011) 25242.

[14] X. Meng, A.V. Kildishev, K. Fujita, K. Tanaka and V.M. Shalaev, Nano Lett. **13** (2013) 4106.

[15] K.J. Webb and A. Ludwig, Phys. Rev. B **78** (2008) 153303.

[16] Y. Fu, L. Thylén and H. Agren, Nano Lett. **8** (2008) 1551.

[17] K.J Webb and L. Thylen, Optics Letters, Vol. **33** (2008), 747.

[18] M.A. Malik, P. O'Brien and N. Revaprasadu, Chem. Mater. **14** (2002) 2004.

[19] J.S. Steckel, J.P. Zimmer, S.Coe-Sullivan, N.E. Stott, V. Bulovic and M.D. Bawendi, Angew. Chem. Int. Ed. **43** (2004) 2154.

[20] A. Datta, S.K. Panda and S. Chaudhuri, J. Phys. Chem. **111** (2007) 17260.

[21] J.-H. Song, T. Atay, S. Shi, H, Urabe and A.V. Nurmiko, NanoLetters **5** (2005) 1557.

[22] Y. Ma, H.X. Bai, C. Yang, X.R. Yang, Analyst **130** (2005) 1386.

[23] D.A. Bussian, S.A. Crooker, M. Yin, M. Brynda, AL. Efros and V.I. Kliomov, Nature Materials, **8** (2009) 35.

[24] P. Reiss, J. Bleuse and A. Pron, Nano Lett. **2** (2002) 781.

[25] J. Schrier, D.O. Demchenko, L.-W. Wang and A.P. Alivisatos, Nano Lett. **7** (2007) 2377.

[26] A. Francheschetti, H. Hu, L.W. Wang and A. Zunger, Phys. Rev. B **60** (1999) 1819.

[27] P.G. Bolcatto and C.R. Proetto, Phys. Stat. Sol. (b), **220** (2000) 220.

[28] G. Bester and A. Zunger, Phys. Rev. B, **68** (2003) 73309.

[29] L.-W. Wang and A. Zunger, Phys. Rev. Lett. **73** (1994) 1039.

[30] R.D. Averitt, S.L. Westcott and N.J. Halas, J. Opt. Soc. Am. B, **16** (1999) 1824.

[31] U. Woggon *Optical properties of semiconductor quantum dots* (Springer, Berlin, 1996).

[32] A. Sihvola, Subsurface sensing technologies and applications **1** (2000) 393.

[33] R.M. de la Cruz, C. Kanyinda-Malu and P. Rodríguez, Physica E **44** (2012) 1868.

[34] R.M. de la Cruz and C. Kanyinda-Malu, Physica E **44** (2012) 1250.

[35] F. Demangeot, J. Frandon, M.A. Renucci, C. Meny, O. Briot, and R.L. Aulombard, J. Appl. Phys. **82** (1997) 1305.

[36] P. Holmström, L. Thylén and A. Bratkovsky, Appl. Phys. Lett. **97** (2010) 073110.

[37] L. Martiradonna, M. De Giorigi, L. Troisi, L. Carbone, G. Gligi, R. Ciongolani, M.D. Vittorio, *2006 International Conference on Transport Optical Network, 18-22 June 2006*, Vol. 2, 64 (2006).

[38] J. Brandrup J and E.K. Immergut (ed) *Polymer handbook* (New York:Wiley, 1989).

[39] Landolt-Börnstein *Numerical data and functional relationships in science and technology* (Berlin:Springer, 1982).

[40] P.M. Nikolic, Z. Dinovic, K. Radulovic, D. Vasijevic-Radovic, S. Duric, P. Mihajlovic, D.I. Siapkas, and T.T. Zorba *Proc. 22nd International Conference on Microelectronics* (Miel, 2000), Vol. 1, Nis, Serbia.

[41] A.G. Rolo, L.G. Vieira, M.J.M. Gomes, J.L. Ribeiro, M.S. Belsley and M.P. dos Santos, Thin solid films **312** (1998) 348.

[42] A. Bratkovsky, E. Pomzovskaya, S.-Y. Wang, P. Holmström, L. Thylén, Y. Fu and H. Agren, Appl. Phys. lett. **93** (2008) 193106.

[43] A. Yariv, *Quantum Electronics*, 3rd ed: Wiley, New York 1989, p 237.

[44] X. Wang, X. Ren, K. Kahen, M.A. Hahn, M. Rajeswaran, S. Maccagnano-Zacher, J. Silcos, G.E. Cragg, A.L. Efros and T.D. Krauss, Nature Letters. doi:10.1038/nature08072, 1 (2009).

[45] R.M. de la Cruz, S.W. Teitsworth and M.A. Stroscio, Superlatt. and Microstruct. **13**, 481 (1993).